JOC The Journal of Organic Chemistry

Article

pubs.acs.org/joc

Unexpected, Latent Radical Reaction of Methane Propagated by Trifluoromethyl Radicals

Nima Zargari,[†] Pierre Winter,[‡] Yong Liang,[§] Joo Ho Lee,[†] Andrew Cooksy,*[,‡] K. N. Houk,*[,§] and Kyung Woon Jung*[,†]

[†]Loker Hydrocarbon Research Institute, Department of Chemistry, University of Southern California, 837 Bloom Walk, Los Angeles, California 90089, United States

[‡]Department of Chemistry and Biochemistry, San Diego State University, 5500 Campanile Drive, San Diego California 92182, United States

[§]Department of Chemistry and Biochemistry, University of California, Los Angeles, California 90095, United States

Supporting Information

ABSTRACT: Thorough mechanistic studies and DFT calculations revealed a background radical pathway latent in metal-catalyzed oxidation reactions of methane at low temperatures. Use of hydrogen peroxide with TFAA generated a trifluoromethyl radical ($\bullet CF_3$), which in turn reacted with methane gas to selectively yield acetic acid. It was found that the methyl carbon of the product was derived from methane, while the carbonyl carbon was derived from TFAA. Computational studies also support these findings, revealing the reaction cycle to be energetically favorable.

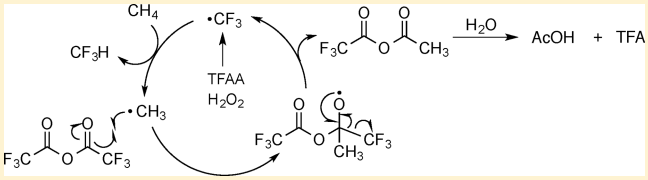

INTRODUCTION

Methane, in the form of natural gas, is the most abundant hydrocarbon but the least reactive due to its high bond dissociation energy.[1] Because methane and its flared product, carbon dioxide, are major greenhouse gases,[2] it is of paramount importance to discover novel ways to functionalize methane. Various oxidants with transition metals or even main group catalysts have been investigated in order to oxidize methane into chemical feedstock products with varying degrees of success.[3] Seminally, Sen, Mizuno, and Ingrosso used hydrogen peroxide in trifluoroacetic acid (TFA) and trifluoroacetic anhydride (TFAA) to successfully convert methane gas to either methyl trifluoroacetate or acetic acid as major liquid products.[4−6] Despite low yields based on methane, these methodologies were progressive and pioneering. These transformations required the use of transition metal catalysts; however, their mechanisms including the possible presence of nonmetallic background processes were not comprehensively studied. Herein, we report a background reaction which we have identified as a radical process.[7] The purpose of this paper is to provide clarity to the mysterious and underdeveloped reaction of methane gas under radical conditions in TFA and TFAA solution.

Using various palladium catalysts including our NHC-amidate complex,[8] we examined the oxidation of methane under conditions similar to those in the work done by Sen at 90 °C and obtained methanol in yields similar to those Sen reported. However, at lower temperatures (60 °C), we observed acetic acid as the primary product. To our surprise, the same amount of acetic acid was seen without the use of any palladium catalysts, as well. As depicted in Scheme 1, acetic acid was selectively generated from methane at 60 °C, while we also observed the presence of another critical product, fluoroform, which stemmed from TFA/TFAA (vide infra). Hence, we embarked on the study of this background reaction to better understand the mechanistic pathway.

Scheme 1. Background Radical Reaction at a Low Temperature

$$CH_4 \xrightarrow[60\ ^\circ C,\ 16\ h]{TFAA,\ TFA,\ H_2O_2} \underset{3.8\%}{CH_3CO_2H} + \underset{0.6\%}{CF_3H}$$

RESULTS AND DISCUSSION

In the absence of methane, no products were observed, indicating that methane was the actual carbon source for the intended reactions. When we employed ^{13}C-labeled methane, we observed acetic acid as the only meaningful ^{13}C incorporating product (Figure 1). However, the acetyl protons in the ^{1}H NMR spectra exhibited a large one-bond ^{13}C−H coupling (J_{C-H} = 130 Hz) but no two-bond coupling (i.e., ^{13}C−^{13}C−H), signaling that only the methyl of the acetyl group came from methane. In addition, fluoroform was constantly detected in variable amounts, suggesting that the C−C bond of the trifluoroacetyl group was cleaved to offer the carbonyl

Received: August 4, 2016
Published: September 29, 2016

DOI: 10.1021/acs.joc.6b01903
J. Org. Chem. 2016, 81, 9820−9825

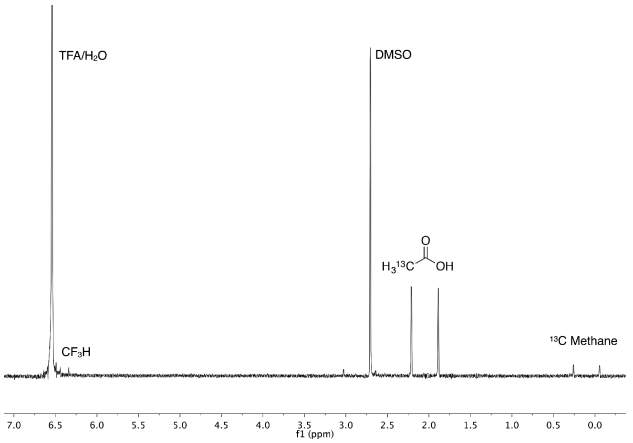

Figure 1. Wet1D ^{1}H NMR of ^{13}C-labeled methane reaction (DMSO was added as an internal NMR standard after the reaction).

moiety, which would be incorporated into the produced acetic acid (vide infra).

In the proton-coupled ^{13}C NMR spectra (Figure 2), similar patterns were demonstrated, where the methyl carbon of the

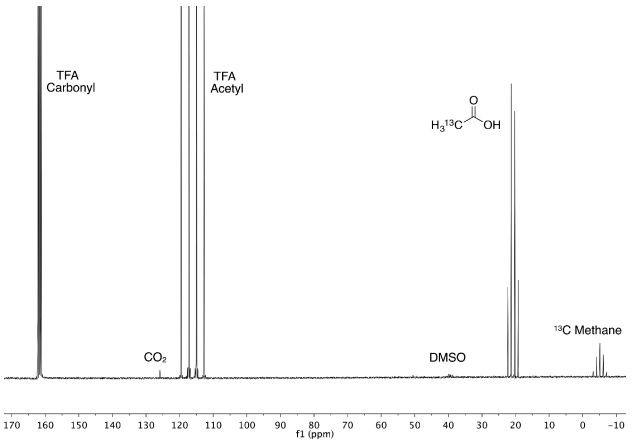

Figure 2. ^{13}C NMR of ^{13}C-labeled methane reaction (DMSO was added as an internal NMR standard after the reaction).

acetyl group showed a quartet with a large coupling constant due to the aforementioned one-bond coupling (J_{C-H} = 130 Hz). The carbonyl carbon peak was negligible due to low abundance of ^{13}C, suggesting this carbon would be naturally abundant ^{12}C. Both spectrum data confirmed that methane was a key reactant to form the methyl portion of acetic acid, and the carbonyl moiety would stem from another carbon source.

As a potential candidate of the extra carbon sources, we first decided to see if carbon dioxide would react since we usually detected carbon dioxide in small amounts (Figure 2). However, the addition of either carbon dioxide or carbon monoxide did not affect the yield of the reaction. Thus, it was concluded that TFAA/TFA would offer the carbonyl moiety to the produced acetic acid since they were the only carbon-containing compounds left in the reaction mixture.

We investigated the effect of TFA and TFAA in order to determine which reagent participated in the formation of acetic acid and fluoroform (Table 1). The reaction did not proceed when TFAA was excluded (entry 1). As the amount of TFAA increased, the reaction afforded higher yields of acetic acid and smaller quantities of methanol (entries 2−4). Use of pure

Table 1. Effects of TFAA and TFA[a]

entry	TFAA/TFA (mmol)	AcOH (μmol, yield)	MeOH (μmol)
1	0.0/11		
2	1.4/8.1	33 (1.0%)	2.0
3	2.8/5.4	55 (1.7%)	0.7
4	4.3/2.7	121 (3.8%)	
5	5.7/0.0	25 (0.77%)	

[a]Reaction conditions: varying amounts of TFAA and TFA were added to 130 μmol of 30% H_2O_2 in a stainless steel reactor with a high-pressure valve and charged with 3200 μmol of methane. The mixture was stirred at 60 °C for 16 h. D_2O was added to the reaction mixture, and a wet1D NMR was taken using DMSO as an internal standard. Yields were calculated based on methane as the limiting reagent.

TFAA resulted in a lower yield, suggesting acidic anhydrous conditions are required (entry 5). These results supported the role of TFAA rather than TFA as the carbonyl source of the observed acetic acid. The necessity of having an excess amount of TFAA has significant mechanistic implications, which include the trapping of acetic acid within a mixed anhydride (vide infra).

Since CF_3H was observed in both ^{1}H and ^{19}F NMR, we proposed that the trifluoromethyl radical ($\bullet CF_3$) would be the chain carrier of this reaction. In conditions including hydrogen peroxide and TFAA, there are several ways in which $\bullet CF_3$ can be produced. As depicted in Scheme 2, the radical processes

Scheme 2. Formation of Trifluoroperacetic Acid and Subsequent Reaction with Methane

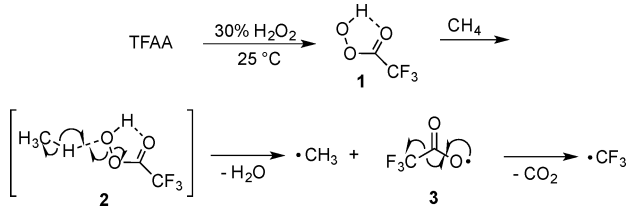

can be initiated by trifluoroperacetic acid **1** (TFPAA), which is in accordance with previous studies performed with TFAA and hydrogen peroxide at room temperature.[9] Therefore, TFPAA (**1**) can react directly with methane to form intermediate **2**.[10] Radical degradation of this complex would furnish methyl ($\bullet CH_3$) and TFA radicals (**3**) along with water. Decarboxylation of TFA radical **3** leads to the facile production of trifluoromethyl radical ($\bullet CF_3$), which plays a crucial role in the subsequent radical propagation processes. Previous studies also confirmed that trifluoroacetyl peroxides furnished fluoroform along with carbon dioxide when they were subjected to thermal decomposition in hydrocarbon solvents.[11]

Another source of $\bullet CF_3$ is bis(perfluoroacetyl) peroxide **4** (Scheme 3). When hydrogen peroxide is added to a solution of TFAA and trace amounts of base, **1** is no longer produced and the primary product is bis(perfluoroacetyl) peroxide **4**.[9] Alternatively, when 30% hydrogen peroxide is introduced dropwise into a biphasic system of an aqueous alkaline media and Freon 113, **4** is also produced.[12] At increased temperatures, **4** readily undergoes homolysis, and the resulting TFA radical **3** rapidly dissociates to give rise to the formation of trifluoromethyl radical ($\bullet CF_3$).

Our standard reaction conditions were applied using all three different pathways of producing trifluoromethyl radical initiators and all produced acetic acid as the selective product.

DOI: 10.1021/acs.joc.6b01903
J. Org. Chem. 2016, 81, 9820−9825

Scheme 3. Formation of Bis(perfluoroacetyl) Peroxide and Subsequent Homolysis

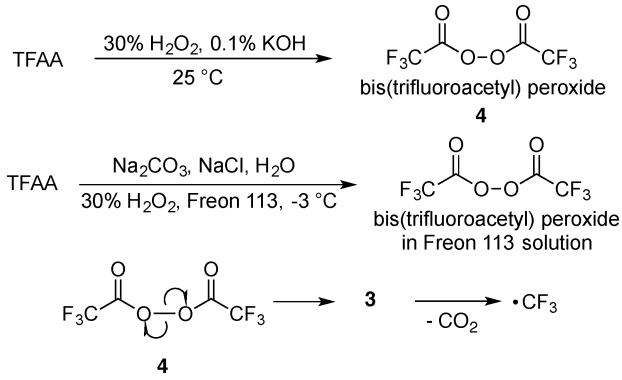

Most importantly, in the reaction in which bis(perfluoroacetyl) peroxide in Freon 113 solution was used as the trifluoromethyl radical initiator, no additional hydrogen peroxide was introduced into the solution. This supports our belief that the radical chain carrier of this methane functionalization reaction is the trifluoromethyl radical ($\bullet CF_3$).

The ^{19}F NMR of the solutions prior to reacting them with methane clearly showed the selective formation of either **1** or **4** (Figure 3). Since our standard reaction conditions did not use

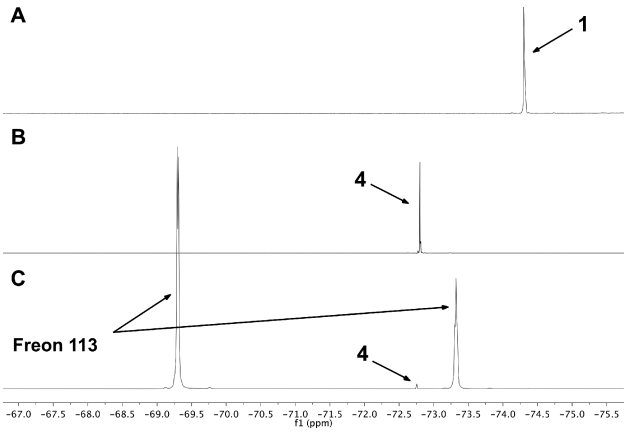

Figure 3. ^{19}F NMR of three methods of forming trifluoromethyl radical sources: (A) addition of H_2O_2 to a TFA/TFAA solution at room temperature; (B) addition of H_2O_2 to a TFA/TFAA solution with trace amounts of potassium hydroxide at room temperature; (C) dropwise addition of H_2O_2 into a biphasic system of an aqueous alkaline media and Freon 113 at −4 °C.

any bases, trifluoroperacetic acid **1** (TFPAA) would be the trifluoromethyl radical source of the reactions, not bis-(perfluoroacetyl) peroxide **4**.

As illustrated in Scheme 4, trifluoromethyl radical ($\bullet CF_3$) reacts with methane to form a methyl radical ($\bullet CH_3$) and fluoroform (CF_3H) because of the favorable difference in the bond dissociation energies between fluoroform (446.4 kJ/mol) and methane (439.7 kJ/mol).[13] After the produced methyl radical ($\bullet CH_3$) adds to TFAA, the resultant intermediate **5** undergoes radical dissociation to mixed anhydride **6**, while trifluoromethyl radical ($\bullet CF_3$) is regenerated to propagate the radical cycle. Upon treatment with water during the workup, mixed anhydride **6** is ultimately liberated into acetic acid and TFA. This mechanistic scheme is similar to the one proposed by Sen while investigating the radical-initiated oxidative

Scheme 4. Methane Functionalization by Proposed Radical Processes and Termination of Trifluoromethyl Radical

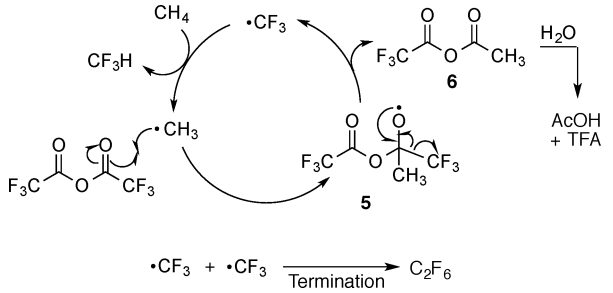

functionalization of higher chain alkanes such as ethane and propane.[4b] Interestingly, the trifluoromethyl radical might add to TFAA; however, we did not observe other potential dissociation products such as hexafluoroacetone. The adduct would dissociate to $\bullet CF_3$ more rapidly *via* the reversible process of the addition than the dissociation of the anhydride C−O bond to hexafluoroacetone. Termination of this radical process may occur by the reaction of two trifluoromethyl radicals ($\bullet CF_3$), forming hexafluoroethane (C_2F_6), which was observed in ^{19}F NMR. Hexafluoroethane is commonly seen as a decomposition product of reactions containing trifluoromethyl radicals ($\bullet CF_3$).[14]

This mechanistic approach takes into account several critical observations. First, greater amounts of acetic acid were observed as the amount of TFAA increased because TFAA provided both CF_3 radical as the reagent and the carbonyl group as the substrate. Second, acetic acid was not detected until the aqueous workup because the mixed anhydride **6** was stable during the reaction conditions. As a consequence, at low temperatures, the overoxidation of acetic acid to carbon dioxide was inhibited, while higher temperatures may have degraded the mixed anhydride. The rare cases where trace methanol was observed may be caused by the direct oxidation of methane via peroxide radicals. Finally, since water could be formed as a byproduct of the radical degradation of complex **2** (Scheme 2), excess amounts of TFAA were used to maintain anhydrous reaction conditions.

Seeking evidence to corroborate the proposed mechanism, we carefully analyzed products by using NMR and GC methods mainly to identify important product species such as fluoroform, hexafluoroethane, carbon dioxide, and mixed anhydride **6**. We confirmed the presence of fluoroform by both wet1D ^1H (Figure 1) and ^{19}F NMR. Hexafluoroethane was observed as another fluorine-containing product besides fluoroform by ^{19}F NMR analysis. By employing wet1D ^1H and ^{13}C NMR techniques, we detected the mixed anhydride at the end of the reaction as well as its rapid hydrolysis to acetic acid and TFA upon the addition of water. Under standard reaction conditions (Table 1, entry 4), proton-coupled ^{13}C NMR studies (Figure 2) showed the production of carbon dioxide, while gas chromatography analysis quantified the amount to be 109 μmol. These results suggested that 130 μmol of hydrogen peroxide led to 109 μmol of CO_2 and the equimolar amount of trifluoromethyl radical ($\bullet CF_3$). Acetic acid as the only liquid product was obtained in slightly larger amounts (i.e., 121 μmol), implying the radical cycle proposed in Scheme 4 would be in play.

Rigorous computational studies were also performed to support these experimental findings. The radical processes for

DOI: 10.1021/acs.joc.6b01903
J. Org. Chem. 2016, 81, 9820−9825

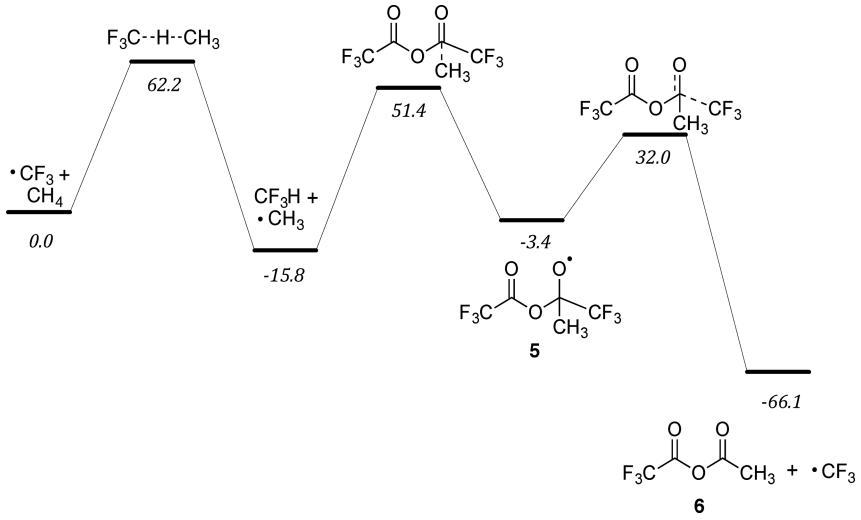

Figure 4. TFA-solvated relative free energy (kJ/mol) diagram for Scheme 4 reactions. Vibrational corrections were calculated at 333 K and 27.0 atm.

methane functionalization in Scheme 4, with the exception of the hydrolysis of mixed anhydride **6** and the radical termination reaction, were analyzed computationally using Gaussian 09.[15] The bimolecular reaction between the trifluoromethyl radical ($\bullet CF_3$) and methane will be referred to as reaction 1. The bimolecular addition reaction between the methyl radical ($\bullet CH_3$) and TFAA will be referred to as reaction 2. Finally, the unimolecular decomposition reaction of **5** into trifluoromethyl radical and **6** will be referred to as reaction 3. Each of these reactions proceeds through a single transition state which will be referred to as transition states 1, 2, and 3, respectively.

The COSMO model was used to estimate the solvent effects of TFA on the single-point energies of all reactants, transition states, and products. The COSMO results predict that the free energies of reaction for reactions 1 and 3 are both lowered by 7.7 kJ/mol when using TFA as a solvent but increase by 1.8 kJ/mol for reaction 2. For reactions 2, the energy of activation did not change significantly when using the COSMO model. The free energies of activation for reactions 1 and 3, however, were each reduced by 3.0 kJ/mol when the COSMO model was employed. From these data, we conclude that solvation plays an important role in the reaction thermodynamics of Scheme 4 if not the kinetics (Figure 4).

Frequency calculations were performed on the optimized geometries to obtain zero-point and thermal corrections at 333 K and 27.0 atm. These calculations also confirm that our transition state geometries are first-order saddle points and that our reactant and product geometries are minima on the potential energy surface. The single imaginary frequency calculated for each transition state was verified to correspond to the reaction coordinate for that step.

The transfer of a hydrogen atom to proceed from $\bullet CF_3$ and CH_4 to CF_3H and $\bullet CH_3$ is found to occur through transition state 1 (Figure 5). The C−H bond length in this structure is 1.37 Å between $\bullet CF_3$ and the shared hydrogen atom and 1.33 Å between $\bullet CH_3$ and the shared hydrogen atom. The FCH bond angle is 109.8°, and the HCH bond angle is 104.3°. The solvated free energy of activation for this transition state was found to be 62.2 kJ/mol.

Of the three reactions modeled, the transition state for reaction 2 has the highest solvated activation free energy of 67.2 kJ/mol, indicating that this is the slowest reaction in the mechanism. The C−C bond distance in this structure is 2.22 Å

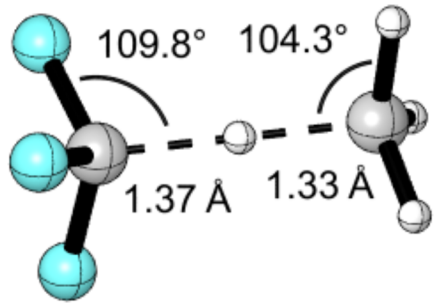

Figure 5. Transition state structure of the reaction between trifluoromethyl radical ($\bullet CF_3$) and methane; carbon, gray; hydrogen, white; and fluorine, blue (reaction 1).

between the carbonyl of TFAA and the $\bullet CH_3$ carbon atom. The CCO bond angle between the previously mentioned carbon atoms and the respective carbonyl oxygen atom is 100.5° (Figure 6).

The structure of transition state 3 shows the removal of the $\bullet CF_3$ group from the reactant to form the mixed anhydride product (Figure 7). The C−C bond length in this structure is

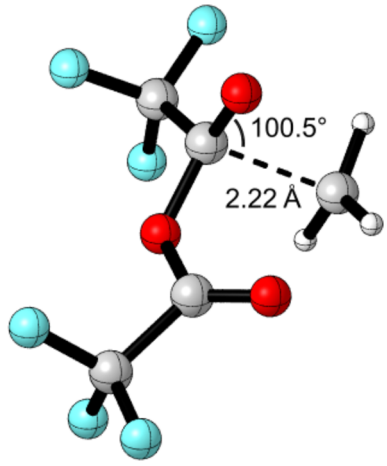

Figure 6. Transition state structure of reaction between the methyl radical ($\bullet CH_3$) and TFAA; carbon, gray; hydrogen, white; oxygen, red; and fluorine, blue (reaction 2).

DOI: 10.1021/acs.joc.6b01903
J. Org. Chem. 2016, 81, 9820−9825

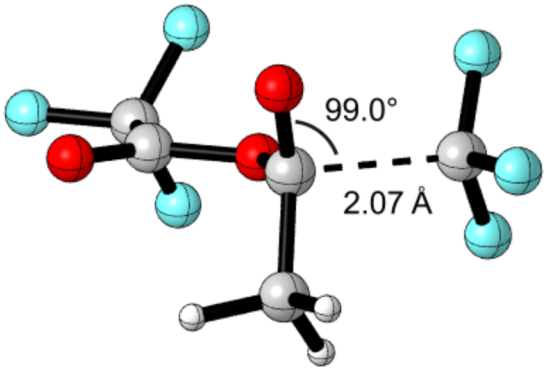

Figure 7. Transition state structure of decomposition reaction of **5** into trifluoromethyl radical and **6**; carbon, gray; hydrogen, white; oxygen, red; and fluorine, blue (reaction 3).

2.07 Å between $\bullet CF_3$ and the carbonyl carbon of the mixed anhydride. The CCO bond angle between the $\bullet CF_3$ moiety and the carbonyl group is 99.0°. The solvated free energy of activation for this transition state was found to be 35.4 kJ/mol.

In an effort to validate the radical process, we evaluated the feasibility of the methane functionalization by using various radical inhibitors and promoters (Table 2). When various radical inhibitors and initiators including butylated hydroxytoluene (BHT), TEMPO, and azobis(isobutyronitrile) (AIBN) were added (10 mol % to hydrogen peroxide), yields of acetic acid were reduced by 75% (entries 2–4 vs entry 1). As expected, a stoichiometric amount of BHT shut down the reaction completely (entry 5). When radical initiators such as AIBN were solely utilized in the absence of hydrogen peroxide, no products were observed. These data support a radical mechanism through the necessity of TFPAA (**1**).

Table 2. Effects of Radical Inhibitors and Initiators

entry	H_2O_2 (μmol)	additive	AcOH (μmol)	MeOH (μmol)
1	130		121	
2	130	BHT[a]	34	1.4
3	130	TEMPO[a]	22	2.1
4	130	AIBN[a]	46	4.3
5	130	BHT[b]		

[a]13 μmol. [b]130 μmol. Reaction conditions: 2.7 mmol TFA, 4.25 mmol TFAA, 130 μmol of 30% H_2O_2; varying amounts of a radical inhibitor and initiator were added to a stainless steel reactor with a high-pressure valve and charged with 3200 μmol of methane. The mixture was stirred at 60 °C for 16 h. D_2O was added to the reaction mixture, and a wet1D NMR was taken using DMSO as an internal standard.

As represented in Table 3, we varied the amounts of hydrogen peroxide and compared the aforementioned results (shown again in Table 3, entry 2). Reducing the amount of hydrogen peroxide by half produced acetic acid in a lower yield as expected (entry 1). However, doubling the amount of hydrogen peroxide failed to furnish additional acetic acid (entry 3). Both of these modified amounts of hydrogen peroxide produced methanol in trace amounts. Therefore, there seemed to be an appropriate stoichiometry between hydrogen peroxide and TFAA for optimal radical processes (entry 2).

CONCLUSION

In summary, we found a background radical reaction latent in metal-catalyzed oxidative functionalizations of methane. Hydrogen peroxide together with TFAA produced the trifluoromethyl radical ($\bullet CF_3$) by trifluoroperacetic acid **1**, though it was also shown that $\bullet CF_3$ can also be produced by the homolysis of bis(perfluoroacetyl) peroxide **4**. The $\bullet CF_3$, in turn, reacted with methane in a favorable reaction, forming fluoroform and methyl radical. The resulting methyl radical reacted with TFAA to generate a mixed anhydride, which was subsequently hydrolyzed into acetic acid. NMR data indicated that the methyl group of acetic acid originated from methane and the carbonyl carbon originated from TFAA. Experimental results from the use of radical initiators and inhibitors along with careful analysis of products and intermediates supported our hypothesis on a radical mechanism. Though similar reaction conditions for methane oxidation have frequently been employed, a thorough study of this intriguing background reaction has not been performed. Thus, we hope that this report will bring some clarity to radical transformations and metal-catalyzed oxidations of methane, the most abundant carbon source.

Table 3. Effect of Hydrogen Peroxide Used[a]

entry	H_2O_2 (μmol)	AcOH (μmol, yield)	MeOH (μmol)
1	65	75 (2.4%)	1.9
2	130	121 (3.8%)	
3	260	109 (3.4%)	1.8

[a]Reaction conditions: 2.7 mmol TFA and 4.25 mmol TFAA were added to varying amounts of 30% H_2O_2 and were added to a stainless steel reactor with a high-pressure valve and charged with 3200 μmol of methane. The mixture was stirred at 60 °C for 16 h. D_2O was added to the reaction mixture, and a wet1D NMR was taken using DMSO as an internal standard.

EXPERIMENTAL SECTION

Methods. All glassware and reactor components were oven-dried prior to use. All chemicals were purchased as reagent grade and used without further purification. ^1H (400 or 500 MHz), ^{13}C (126 MHz), and ^{19}F (470 MHz) NMR spectra were referenced to DMSO or TFA.

A TCD detector for gas chromatography was set at 160 °C, and the inlet temperature was set at 200 °C. Initial oven temperature was 40 °C for 1 min and was then ramped to 50 °C at 10 °C/min. The flow rate was set to 3 mL/min by an argon high-purity carrier. After the reaction was complete, the reactor was cooled at −20 °C for 30 min. The vessel was opened, and the expelled gas was passed through potassium hydroxide and Drierite and collected in a screw cap vial with septum. Resulting gas was then injected into the GC column.

General Method for Methane Functionalization. To a 0.5 dram vial equipped with a stir bar was added a solution of 0.2 mL (2.69 mmol) of TFA, 0.6 mL (4.25 mmol) of TFAA, and 13 μL (130 μmol) of 30% H_2O_2. The solution was stirred at room temperature for 1 min. The reaction was then placed in a stainless steel reactor with a high-pressure valve and was subjected to eight purge cycles and charged with 27 psi (3200 μmol) methane gas. The reactor was stirred at 60 °C for 16 h. The reaction vessels were then held at −20 °C for 30 min. Next, 0.5 mL of D_2O was added to the reaction mixture, and a wet1D NMR was taken using DMSO as an internal standard.

Synthesis of Bis(perfluoroacetyl) Peroxide (4). Sodium carbonate (0.21 g, 2.0 mmol) and sodium chloride (0.11 g, 2.0 mmol) were added to 1.9 mL of deionized water, and the reaction was stirred at 0 °C for 5 min. Next, 0.2 mL of 30% H_2O_2 (20 mmol) and 1.9 mL of Freon 113 were added to the aqueous solution and stirred at −3 °C for 5 min. Then, 0.35 mL (2.5 mmol) of TFAA was added dropwise over 30 min. The organic layer was separated, and ^{19}F NMR was taken using trifluorotoluene as an internal standard: ^{19}F NMR δ −72.76 ppm.

Gaussian Parameters. In all cases, the reactant, product, and transition state geometries were optimized using the B3LYP hybrid functional[16] and Dunning's aug-cc-pVDZ basis set.[17] Diffuse functions

DOI: 10.1021/acs.joc.6b01903
J. Org. Chem. 2016, 81, 9820–9825

were included in the basis set in order to account for long-range interactions, particularly between the fluorine and carbon atoms.

COSMO Paramenrts. Energies were calculated for the gas-phase-optimized geometries both with and without the conductor-like polarizable continuum solvent model (COSMO).[18] Values for the dielectric constant and solute radius were manually configured in Gaussian to most accurately represent TFA.

■ ASSOCIATED CONTENT

Supporting Information

The Supporting Information is available free of charge on the ACS Publications website at DOI: 10.1021/acs.joc.6b01903.

Experimental procedures, computational data, spectroscopic data, copies of wet1D ^{1}H, ^{13}C, and ^{19}F spectra, and gas chromatography data (PDF)

■ AUTHOR INFORMATION

Corresponding Authors

*E-mail: acooksy@mail.sdsu.edu.
*E-mail: houk@chem.ucla.edu.
*E-mail: kwjung@usc.edu.

Notes

The authors declare no competing financial interest.

■ ACKNOWLEDGMENTS

We acknowledge Dr. Richard Giles for helpful discussion as well as the Hydrocarbon Research Foundation, the NIH (S10 RR025432), and the NSF (Grant CHE-1361104) for generous financial support.

■ REFERENCES

(1) Blanksby, S. J.; Ellison, G. B. *Acc. Chem. Res.* **2003**, *36*, 255−263.

(2) (a) Karacan, C. Ö.; Ruiz, F. A.; Cotè, M.; Phipps, S. *Int. J. Coal Geol.* **2011**, *86*, 121−156. (b) Jorgenson, A. K. *Soc. Forces.* **2006**, *84*, 1779−1798. (c) Augenstein, D. *Global Environ. Change.* **1992**, *2*, 311−328. (d) Lashof, D. A.; Ahuja, D. R. *Nature* **1990**, *344*, 529−531. (e) Parkyns, N. D. *Chem. Br.* **1990**, *26*, 841−844.

(3) (a) Fu, R.; O'Reilly, M. E.; Nielsen, R. J.; Goddard, W. A., III; Gunnoe, T. B. *Chem. - Eur. J.* **2015**, *21*, 1286−1293. (b) Guo, Z.; Liu, B.; Zhang, Q.; Deng, W.; Wang, Y.; Yang, Y. *Chem. Soc. Rev.* **2014**, *43*, 3480−3524. (c) Hashiguchi, F. G.; Konnick, M. M.; Bischof, S. M.; Gustafson, S. J.; Devarajan, D.; Gunsalus, N.; Ess, D. H.; Periana, R. A. *Science* **2014**, *343*, 1232−1237. (d) Gupta, S.; Kirillova, M. V.; da Silva, M. F. C. G.; Pombeiro, A. J. L.; Kirillov, A. M. *Inorg. Chem.* **2013**, *52*, 8601−8611. (e) Silva, T. F. S.; Mac Leod, T. C. O.; Martins, L. M. D. R. S.; da Silva, M. F. C. G.; Schiavon, M. A.; Pombeiro, A. J. L. *J. Mol. Catal. A: Chem.* **2013**, *367*, 52−60.

(4) (a) Kao, L. C.; Hutson, A. C.; Sen, A. *J. Am. Chem. Soc.* **1991**, *113*, 700−701. (b) Hogan, T.; Sen, A. *J. Am. Chem. Soc.* **1997**, *119*, 2642−2646.

(5) Seki, Y.; Min, J. S.; Misono, M.; Mizuno, N. *J. Phys. Chem. B* **2000**, *104*, 5940−5944.

(6) Ingrosso, G.; Midollini, N. *J. Mol. Catal. A: Chem.* **2003**, *204−205*, 425−431.

(7) Radical processes were reported using persulfate and peroxodisulfate: (a) Basickes, N.; Hogan, T. E.; Sen, A. *J. Am. Chem. Soc.* **1996**, *118*, 13111−13112. (b) Lin, M.; Sen, A. *J. Chem. Soc., Chem. Commun.* **1992**, 892−893.

(8) Sakaguchi, S.; Yoo, K. S.; O'Neill, J.; Lee, J. H.; Stewart, T.; Jung, K. W. *Angew. Chem., Int. Ed.* **2008**, *47*, 9326−9329.

(9) Krasutsky, P. A.; Kolomitsyn, I. V.; Carlson, R. M. *Org. Lett.* **2001**, *3*, 2997−2999.

(10) Camaioni, D. M.; Bays, J. T.; Shaw, W. J.; Linehan, J. C.; Birnbaum, J. C. *J. Org. Chem.* **2001**, *66*, 789−795.

(11) Serov, S. I.; Zhurarlev, M. V.; Sass, V. P.; Sokolov, S. V. *J. Org. Chem. USSR (Engl. Transl.)* **1980**, *16*, 1360−1362.

(12) Sawada, H.; Nakayama, M. *J. Fluorine Chem.* **1990**, *46*, 423−431.

(13) McGivern, W. S.; Derecskei-Kovacs, A.; North, S. W. *J. Phys. Chem. A* **2000**, *104*, 436−442.

(14) Kopitzky, R.; Willner, H. *Inorg. Chem.* **2001**, *40*, 2693−2698.

(15) Frisch, M. J.; Trucks, G. W.; Schlegel, H. B.; Scuseria, G. E.; Robb, M. A.; Cheeseman, J. R.; Scalmani, G.; Barone, V.; Mennucci, B.; Petersson, G. A.; Nakatsuji, H.; Caricato, M.; Li, X.; Hratchian, H. P.; Izmaylov, A. F.; Bloino, J.; Zheng, G.; Sonnenberg, J. L.; Hada, M.; Ehara, M.; Toyota, K.; Fukuda, R.; Hasegawa, J.; Ishida, M.; Nakajima, T.; Honda, Y.; Kitao, O.; Nakai, H.; Vreven, T.; Montgomery, J. A., Jr.; Peralta, J. E.; Ogliaro, F.; Bearpark, M.; Heyd, J. J.; Brothers, E.; Kudin, K. N.; Staroverov, V. N.; Kobayashi, R.; Normand, J.; Raghavachari, K.; Rendell, A.; Burant, J. C.; Iyengar, S. S.; Tomasi, J.; Cossi, M.; Rega, N.; Millam, J. M.; Klene, M.; Knox, J. E.; Cross, J. B.; Bakken, V.; Adamo, C.; Jaramillo, J.; Gomperts, R.; Stratmann, R. E.; Yazyev, O.; Austin, A. J.; Cammi, R.; Pomelli, C.; Ochterski, J. W.; Martin, R. L.; Morokuma, K.; Zakrzewski, V. G.; Voth, G. A.; Salvador, P.; Dannenberg, J. J.; Dapprich, S.; Daniels, A. D.; Farkas, Ö.; Foresman, J. B.; Ortiz, J. V.; Cioslowski, J.; Fox, D. J. *Gaussian 09*, revision D.01; Gaussian, Inc.: Wallingford, CT, 2013.

(16) (a) Becke, A. D. *J. Chem. Phys.* **1993**, *98*, 5648−5652. (b) Lee, C.; Yang, W.; Parr, R. G. *Phys. Rev. B: Condens. Matter Mater. Phys.* **1988**, *37*, 785−789. (c) Vosko, S. H.; Wilk, L.; Nusair, M. *Can. J. Phys.* **1980**, *58*, 1200−1211. (d) Stephens, P. J.; Devlin, F. J.; Chabalowski, C. F.; Frisch, M. J. *J. Phys. Chem.* **1994**, *98*, 11623−11627.

(17) (a) Dunning, T. H. *J. Chem. Phys.* **1989**, *90*, 1007−1023. (b) Kendall, R. A.; Dunning, T. H.; Harrison, R. J. *J. Chem. Phys.* **1992**, *96*, 6796−6806. (c) Woon, D. E.; Dunning, T. H. *J. Chem. Phys.* **1993**, *98*, 1358−1371.

(18) (a) Cossi, M.; Rega, N.; Scalmani, G.; Barone, V. *J. Comput. Chem.* **2003**, *24*, 669−681. (b) Barone, V.; Cossi, M. *J. Phys. Chem. A* **1998**, *102*, 1995−2001.

DOI: 10.1021/acs.joc.6b01903
J. Org. Chem. 2016, 81, 9820−9825